Report

Cell Reports

Cholinergic Signals in Mouse Barrel Cortex during Active Whisker Sensing

Graphical Abstract

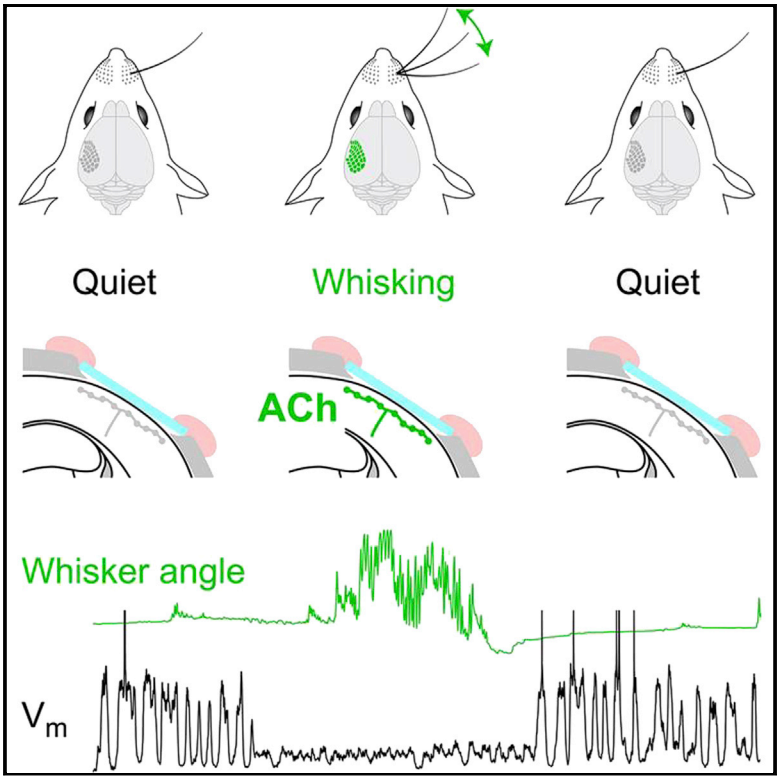

Highlights

Cholinergic axons in the barrel cortex increase activity during whisking

After thalamic inactivation, cholinergic antagonists block whisking cortical state

Optogenetic stimulation of cholinergic neurons mimics the whisking cortical state

Acetylcholine release during whisking acts to suppress slow cortical activity

Authors

Emmanuel Eggermann, Yves Kremer, Sylvain Crochet, Carl C.H. Petersen

Correspondence

sylvain.crochet@epfl.ch (S.C.),
carl.petersen@epfl.ch (C.C.H.P.)

In Brief

Eggermann et al. now find that the desynchronized state of the barrel cortex during active whisker sensing is accompanied by increased cholinergic input, which suppresses slow spontaneous cortical activity in excitatory layer 2/3 barrel cortex neurons.

Eggermann et al., 2014, Cell Reports 9, 1654–1660
December 11, 2014 ©2014 The Authors
http://dx.doi.org/10.1016/j.celrep.2014.11.005

OPEN ACCESS
CellPress

Cell Reports
Report

Cholinergic Signals in Mouse Barrel Cortex during Active Whisker Sensing

Emmanuel Eggermann,[1] Yves Kremer,[1,3] Sylvain Crochet,[1,2,*] and Carl C.H. Petersen[1,2,*]
[1]Laboratory of Sensory Processing, Brain Mind Institute, Faculty of Life Sciences, École Polytechnique Fédérale de Lausanne (EPFL), Lausanne 1015, Switzerland
[2]Co-senior author
[3]Present address: Department of Neuroscience, University of Geneva, Geneva 1211, Switzerland
*Correspondence: sylvain.crochet@epfl.ch (S.C.), carl.petersen@epfl.ch (C.C.H.P.)
http://dx.doi.org/10.1016/j.celrep.2014.11.005

SUMMARY

Internal brain states affect sensory perception, cognition, and learning. Many neocortical areas exhibit changes in the pattern and synchrony of neuronal activity during quiet versus active behaviors. Active behaviors are typically associated with desynchronized cortical dynamics. Increased thalamic firing contributes importantly to desynchronize mouse barrel cortex during active whisker sensing. However, a whisking-related cortical state change persists after thalamic inactivation, which is mediated at least in part by acetylcholine, as we show here by using whole-cell recordings, local pharmacology, axonal calcium imaging, and optogenetic stimulation. During whisking, we find prominent cholinergic signals in the barrel cortex, which suppress spontaneous cortical activity. The desynchronized state of barrel cortex during whisking is therefore driven by at least two distinct signals with opposing functions: increased thalamic activity driving glutamatergic excitation of the cortex and increased cholinergic input suppressing spontaneous cortical activity.

INTRODUCTION

Active mammalian brain states are characterized by desynchronized patterns of cortical activity (Berger, 1929; Buzsáki and Draguhn, 2004; Harris and Thiele, 2011; Lee and Dan, 2012). The somatosensory, visual, and auditory cortices of head-restrained mice transition to an active, desynchronized state when mice are moving compared to the prominent slow, synchronized fluctuations often present when mice are resting (Crochet and Petersen, 2006; Poulet and Petersen, 2008; Gentet et al., 2010; Zagha et al., 2013; Bennett et al., 2013; Polack et al., 2013; Zhou et al., 2014; Schneider et al., 2014).

In the primary somatosensory barrel cortex (S1) of head-restrained mice, slow fluctuations in membrane potential (V_m) are suppressed and excitatory layer 2/3 (L2/3) pyramidal neurons depolarize during active whisker sensing, when the mystacial whiskers are repetitively protracted at high frequency (5–20 Hz) as the mouse scans its immediate facial environment (Crochet and Petersen, 2006). During whisking, the V_m of nearby L2/3 excitatory neurons become less correlated (Poulet and Petersen, 2008). The depolarized and desynchronized V_m define the active cortical state of S1 during whisking. GABAergic neurons in S1 also change their activity during whisking in a cell-type-specific manner. Nonfast spiking GABAergic neurons increase firing rate, whereas parvalbumin-expressing and somatostatin-expressing GABAergic neurons reduce firing rates (Gentet et al., 2010, 2012; Lee et al., 2013). Interestingly, sensory input from the periphery is not necessary for the active cortical state, which therefore appears to be generated by internal brain circuits (Poulet and Petersen, 2008).

The thalamus has been found to play a major role in generating the active state of S1 during whisking. Action potential firing increases in the somatosensory thalamus during whisking, which contributes importantly to driving the depolarized, desynchronized active cortical state (Poulet et al., 2012). However, even after the somatosensory thalamus has been inactivated, there remains a very prominent change in cortical state comparing quiet wakefulness and active whisking periods (Poulet et al., 2012). Thalamic inactivation enhances slow V_m fluctuations during quiet wakefulness, but interestingly nearly all spontaneous activity in L2/3 of S1 is suppressed during whisking after thalamic inactivation. It is therefore clear that there must be other signals, in addition to increased thalamic firing, that contribute to controlling the active whisking-related state of mouse barrel cortex. Here, we demonstrate that the suppression of spontaneous activity in barrel cortex during whisking in thalamic inactivated mice is mediated at least in part by cholinergic signals in S1.

RESULTS

We injected muscimol to inactivate the somatosensory thalamus and then obtained whole-cell V_m recordings from L2/3 neurons in the barrel cortex of awake, head-restrained mice (Poulet et al., 2012). Whisker movements were filmed with a high-speed camera and quantified to correlate with V_m (Crochet and Petersen, 2006; Poulet and Petersen, 2008). Slow V_m fluctuations are prominent in L2/3 neurons of mouse barrel cortex during quiet

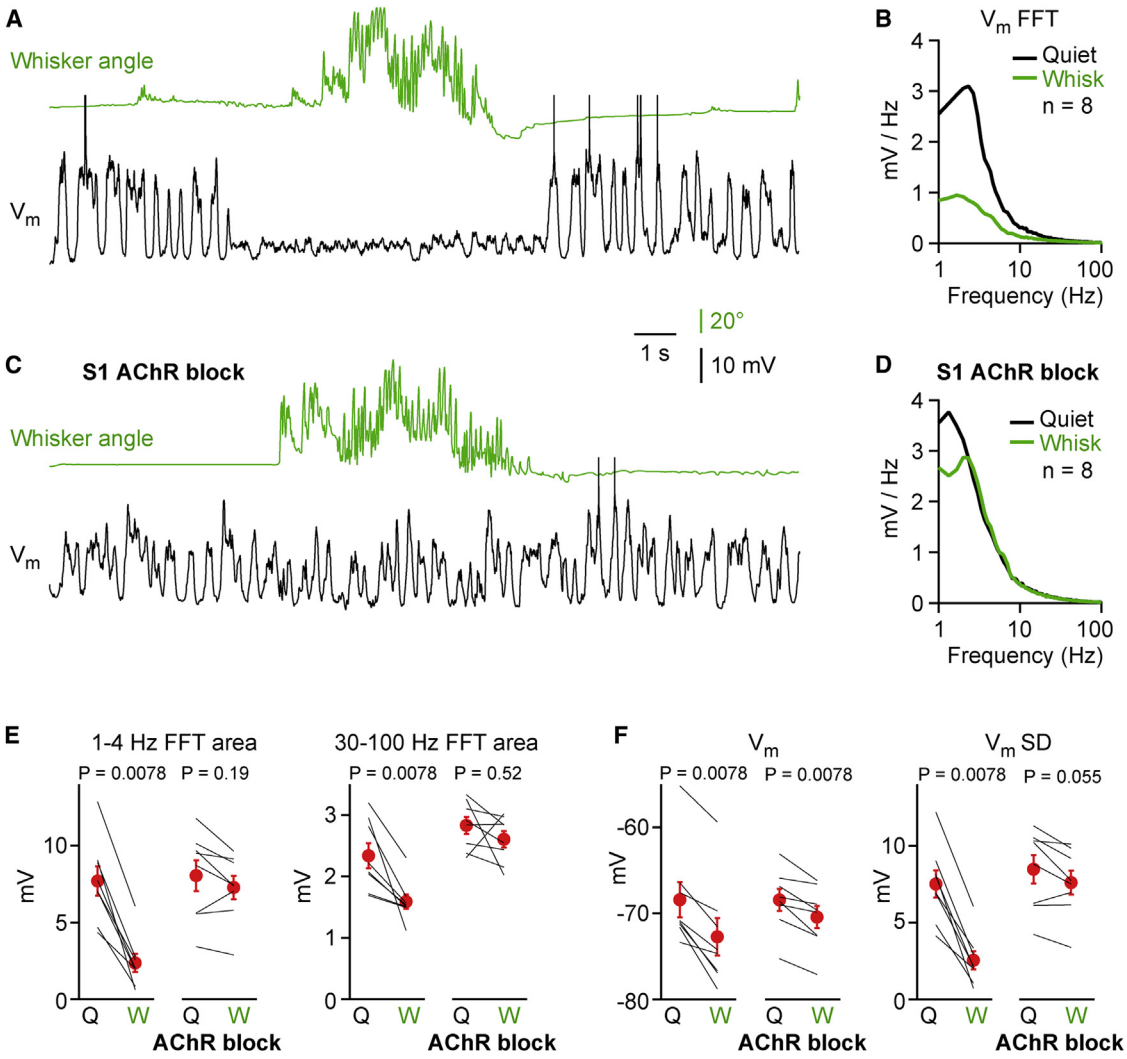

Figure 1. Whisking Correlates with a Change in Cortical State Dependent upon Cholinergic Receptors in Barrel Cortex of Thalamus-Inactivated Mice

(A) V_m (black) of a L2/3 neuron during quantified whisker movement (green).

(B) Grand average FFT of V_m from eight neurons during quiet (black) and whisking periods (green).

(C) V_m and whisker movement after injection of atropine and mecamylamine (AChR blockers) into S1 barrel cortex.

(D) Same as (B), but after blockade of S1 cholinergic receptors in eight other neurons.

(E) Integral 1–4 Hz (left) and 30–100 Hz (right) of V_m FFT during quiet (Q) and whisking (W) periods, before and after blockade of S1 cholinergic receptors.

(F) Mean V_m and SD of V_m.

Lines indicate individual cells and red dots with error bars represent mean ± SEM. APs truncated in (A) and (C). p values are computed with the Wilcoxon signed rank test. See also Figure S1.

wakefulness, when the whiskers are not moving (Figures 1A and 1B) (Poulet et al., 2012). During whisking, both slow and fast V_m oscillations are suppressed ($p = 0.008$, $n = 8$ cells) (Figures 1A, 1B, and 1E), and V_m hyperpolarizes with a reduced SD ($p = 0.008$, $n = 8$ cells) (Figures 1A and 1F) (Poulet et al., 2012). Injection into S1 of pharmacological blockers of cholinergic signaling (atropine to block muscarinic receptors and mecamylamine to block nicotinic receptors) almost completely blocked the whisking-related state change ($n = 8$ cells) (Figures 1C–1F). In thalamus-inactivated mice, the whisking-related suppression of V_m fluctuations and the reduction in V_m variance therefore appear to be caused by increased cholinergic signaling within S1. We observed similar effects in local field potential (LFP) recordings (Figure S1).

Acetylcholine (ACh) is released in the neocortex from axons of neurons with cell bodies located in the basal forebrain (Sarter et al., 2009). To locate cholinergic neurons projecting to S1, we injected green fluorescently labeled choleratoxin subunit B as a retrograde tracer into the C2 barrel column of S1 in transgenic mice with red fluorescently labeled cholinergic neurons (ChAT-Cre × LSL-tdTomato mice) (Madisen et al., 2010; Pinto et al., 2013; Kalmbach and Waters, 2014). We found that cholinergic

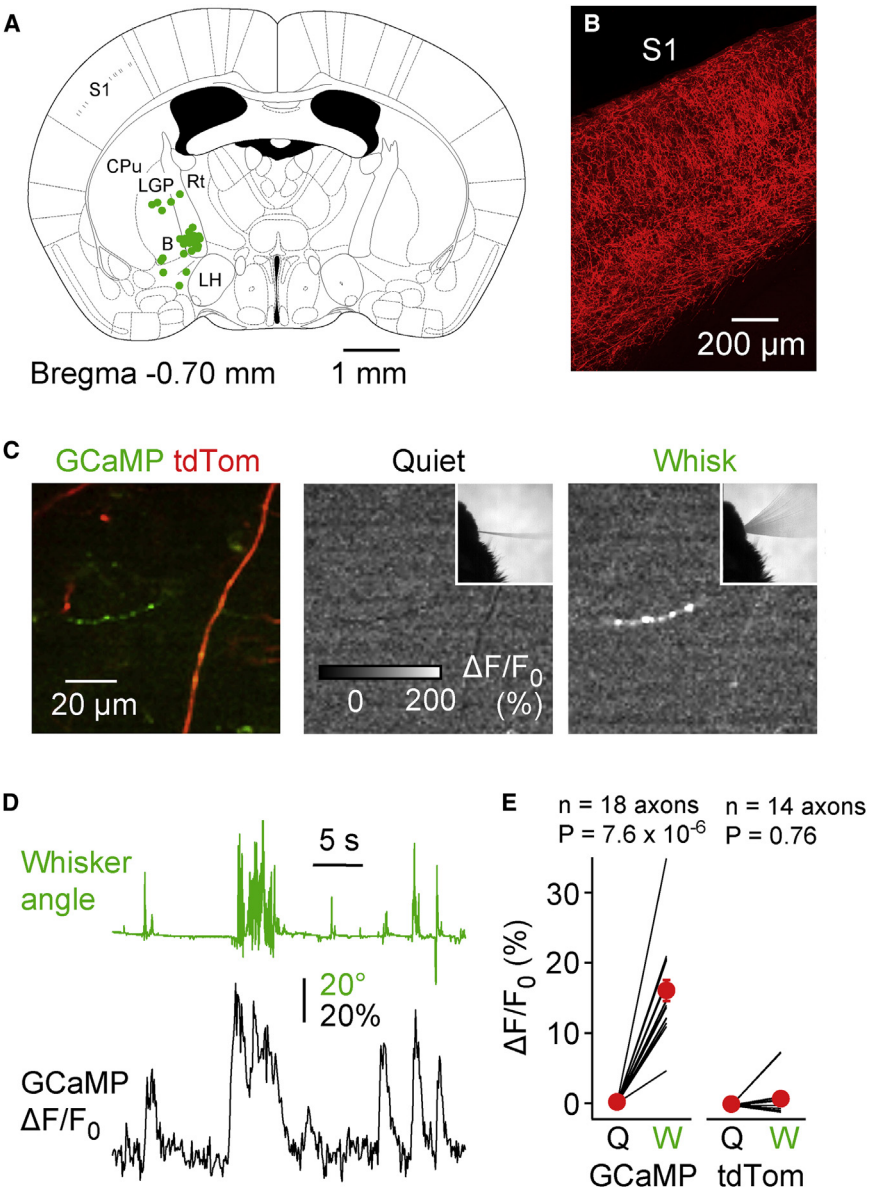

Figure 2. Whisking Correlates with Calcium Signals in Cholinergic Axons in Barrel Cortex

(A) Soma locations of cholinergic neurons projecting to S1 in a ~240-µm-thick coronal slice at ~0.7 mm posterior to Bregma (green dots, superimposed upon a schematic coronal drawing) (Paxinos and Franklin, 2001), retrogradely labeled by the injection of cholera toxin subunit B conjugated to Alexa 488 into the C2 barrel column of a ChAT-Cre × LSL-tdTomato mouse.

(B) Cholinergic axons in S1, labeled by injection of AAV-Flex-tdTomato virus into basal forebrain of a ChAT-Cre mouse.

(C) Two-photon imaging of GCaMP6s (green) and tdTomato (red) expressed in cholinergic axons of S1 (left). Example 2 s average images of fluorescence changes during quiet wakefulness (center) and whisking (right).

(D) Time-course of axon fluorescence changes (black, same GCaMP6s axon as shown in C) during quantified whisker movement (green).

(E) GCaMP6s fluorescence in cholinergic axons of S1 increases significantly during whisking, but red fluorescence (tdTomato) in cholinergic axons does not change.

Lines indicate individual axons, and red dots with error bars represent mean ± SEM. p values are computed with the Wilcoxon signed rank test. See also Figure S2.

neurons projecting to S1 were sparsely distributed in the basal forebrain between Bregma and ~1.8 mm posterior to Bregma (Figures 2A and S2). Selective viral expression of the fluorescent protein tdTomato in the cholinergic neurons of the basal forebrain of ChAT-Cre mice revealed a prominent cholinergic axonal innervation of S1 (Figure 2B). Similarly, we specifically expressed the genetically encoded calcium indicator GCaMP6s (Chen et al., 2013) in basal forebrain cholinergic neurons in order to measure axonal activity in S1 (Petreanu et al., 2012). We then imaged the fluorescence of the cholinergic axons in S1 through a cranial window in awake, head-restrained mice using a two-photon microscope. We found that cholinergic axons expressing GCaMP6s increased fluorescence robustly during whisking periods ($p = 8 \times 10^{-6}$, n = 18 axons in eight mice) (Figures 2C–2E). As a control, we imaged ChAT axons expressing tdTomato and found that this red fluorescence did not change during whisking (p = 0.8, n = 14 axons in five mice) (Figure 2E). Calcium concentration therefore increased in cholinergic axons during whisking, likely causing release of ACh in S1, which might thus activate cholinergic receptors driving the whisking-related suppression of spontaneous activity in the barrel cortex (Figure 1).

Finally, we tested whether optogenetic activation of the cholinergic neurons would be sufficient to drive the cortical state change in thalamus-inactivated mice (Figure 3). We inserted an optical fiber above the location of cholinergic neurons projecting to S1 in ChAT-ChR2 mice (ChAT-Cre × LSL-ChR2) (Kalmbach and Waters, 2014). Blue light during periods without whisking caused suppression of slow and fast V_m fluctuations (p = 0.03, n = 6 cells) (Figures 3A, 3B, and 3E) and hyperpolarization of V_m with reduced SD (p = 0.03, n = 6 cells) (Figures 3A and 3F). These effects were blocked by injection of cholinergic receptor antagonists into S1 (n = 5 cells) (Figures 3C–3F). LFP recordings in S1 showed similar effects (Figure S3). In thalamus-inactivated mice, the cortical state change induced by optogenetic stimulation of cholinergic neurons is therefore very similar to the whisking-related cortical state change (compare Figure 1 and Figure 3).

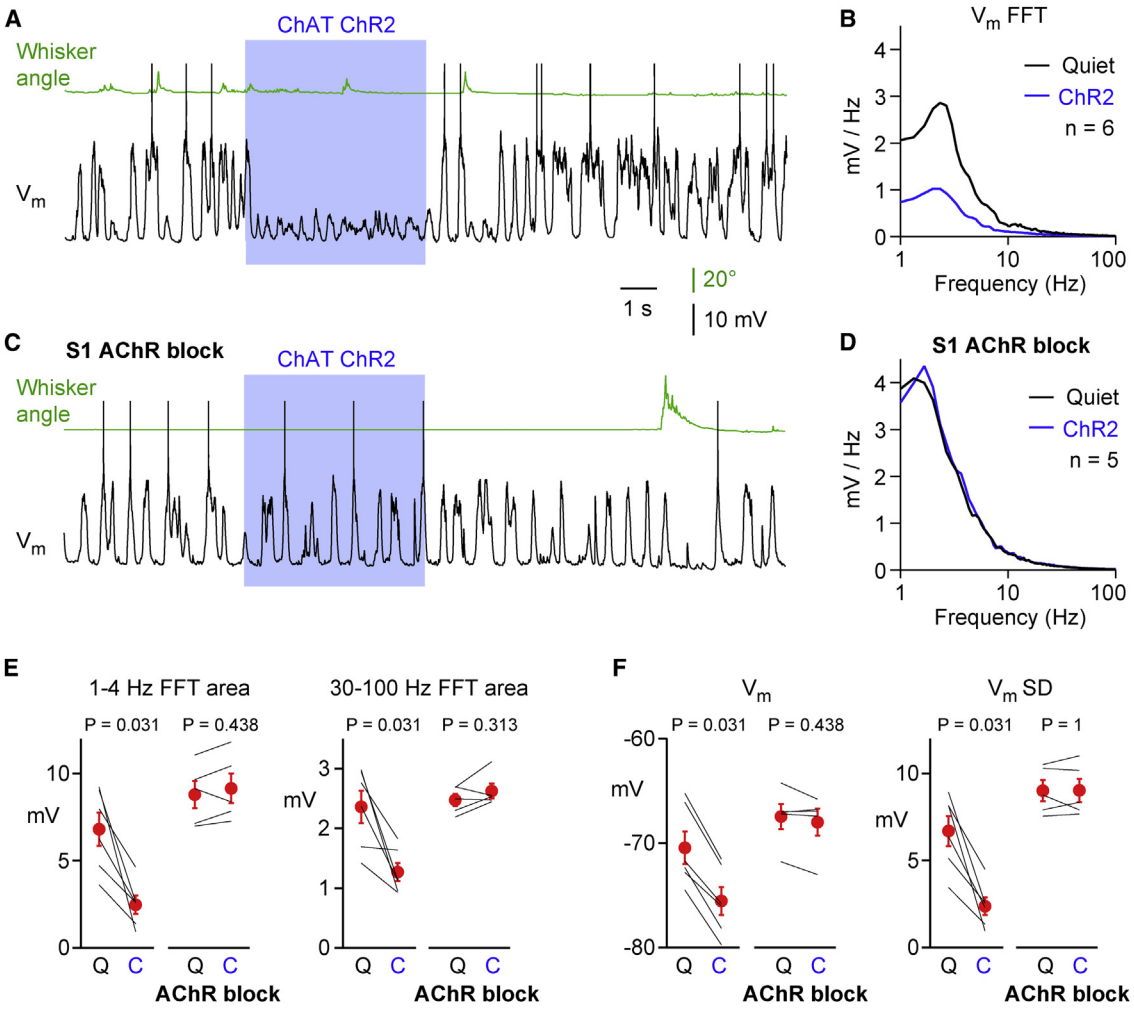

Figure 3. Optogenetic Stimulation of Cholinergic Neurons Induces a Cortical State Change Similar to Whisking

(A) V_m (black) and quantified whisker movement (green) during control period and during blue light illumination to stimulate cholinergic neurons expressing ChR2 (ChAT ChR2) in a thalamus-inactivated mouse.

(B) Grand average FFT of V_m during quiet wakefulness without (black) and with optogenetic stimulation of cholinergic neurons (blue) in six neurons.

(C) Same as (A), but after injection of atropine and mecamylamine into S1 to block cholinergic receptors.

(D) Same as (B), but after blockade of cholinergic receptors in S1 in five other neurons.

(E) Integral over 1–4 Hz (left) and 30–100 Hz (right) of V_m FFT during quiet wakefulness (Q) and during optogenetic stimulation of cholinergic neurons (C), before and after blockade of cholinergic receptors in S1 of thalamus-inactivated mice.

(F) V_m and SD of V_m.

Lines indicate individual cells and red dots with error bars represent mean ± SEM. APs truncated in (A) and (C). p values are computed with the Wilcoxon signed rank test. See also Figure S3.

DISCUSSION

The Active State of Barrel Cortex during Whisking

The desynchronized state of barrel cortex during whisking appears to be composed of at least two distinct signals: increased thalamic activity (Poulet et al., 2012) and increased cholinergic input (Figures 1, 2, and 3). We found that the activity of cholinergic axons correlates with whisking (Figure 2), and, in thalamus-inactivated mice, cholinergic signaling in S1 is both necessary (Figure 1) and sufficient (Figure 3) for the remaining whisking-related cortical state change. The whisking-related release of ACh causes the suppression of spontaneous slow oscillatory activity accompanied by hyperpolarization of L2/3 neurons in S1 (Figures 1 and 3).

Our results in behaving mice are in agreement with in vitro studies of brain slices showing muscarinic suppression of slow activity in S1 (Favero et al., 2012; Wester and Contreras, 2013). The activation of muscarinic receptors can suppress cortical activity by (1) hyperpolarizing excitatory neurons (Eggermann and Feldmeyer, 2009; Gulledge and Stuart, 2005), (2) enhancing neocortical GABAergic inhibition (McCormick and Prince, 1986), and (3) presynaptically inhibiting neurotransmitter release (Gil et al., 1997; Kruglikov and Rudy, 2008; Eggermann and Feldmeyer, 2009; Favero et al., 2012; Wester and Contreras, 2013).

Nicotinic signaling during whisking could also contribute to the active cortical state in S1. Nonfast spiking GABAergic neocortical neurons expressing vasoactive intestinal peptide increase their activity during whisking (Gentet et al., 2010; Lee et al., 2013), in part driven by nicotinic receptor activation (Fu et al., 2014). Vasoactive intestinal peptide-expressing neurons inhibit somatostatin-expressing GABAergic neocortical neurons during whisking (Gentet et al., 2012; Lee et al., 2013; Pfeffer et al., 2013), thereby disinhibiting distal dendrites of excitatory pyramidal neurons, which are prominent locations for long-range cortical input, including excitatory projections from whisker motor cortex (M1) (Matyas et al., 2010; Petreanu et al., 2012). ACh might therefore indirectly contribute to desynchronizing S1 during whisking by promoting excitation from M1 (Lee et al., 2013; Zagha et al., 2013). However, it should be noted that although M1 inactivation affects S1 activity, it does not prevent the cortical state change comparing quiet and active wakefulness (Zagha et al., 2013).

Our recordings were from L2/3 of mouse barrel cortex, and it is possible that cholinergic signaling will differentially affect neurons in different cortical layers (Gulledge et al., 2007; Eggermann and Feldmeyer, 2009). In future studies, it will therefore be important to measure the impact of whisking-related cholinergic signals on the diverse cell types present across different layers of the neocortex.

Cholinergic Signals in Cortex

Cholinergic input to cortex has long been considered to act as a global activating system (Buzsáki et al., 1988; Metherate et al., 1992; Jones 2005). Cholinergic neurons fire at higher rates during wakefulness than slow-wave sleep (Lee et al., 2005) and send widespread axonal collaterals innervating the whole neocortex to release acetylcholine mainly through volume transmission. However, there are currently no direct measurements of cholinergic signaling and cortical state changes on rapid timescales with behavioral relevance in awake mice. Here, we demonstrate prominent cholinergic signals during whisking in S1, and we show that the released acetylcholine suppresses slow spontaneous activity during whisking. Physiologically, the suppression of slow spontaneous activity accompanied by hyperpolarzation in L2/3 of S1 by ACh during whisking is likely to help adjust neocortical network function, counteracting the increased thalamic input during whisking (Poulet et al., 2012). Cholinergic input to S1 cortex might also contribute to the reduced amplitude and spread of whisker-deflection-evoked sensory responses during whisking compared to quiet wakefulness (Crochet and Petersen, 2006; Ferezou et al., 2007).

In addition to its role in controlling cortical states, ACh has been proposed to play important roles in attention (Parikh et al., 2007; Herrero et al., 2008), reward signaling (Chubykin et al., 2013), and learning (Bakin and Weinberger, 1996; Kilgard and Merzenich, 1998). Recently, Pinto et al. (2013) reported enhanced visual perception in mice during cholinergic optogenetic stimulation, with some effects thought to occur through direct action of ACh upon primary visual cortex. In future experiments, it will therefore be of great interest to measure, correlate, and manipulate cholinergic activity and its impact upon S1 during execution and learning of whisker-dependent perceptual tasks in head-restrained mice (O'Connor et al., 2010; Sachidhanandam et al., 2013).

EXPERIMENTAL PROCEDURES

Animals and Surgery

All experiments were carried out with 6- to 12-week-old mice, in accordance with the Swiss Federal Veterinary Office (authorization 1628.3 for awake recordings and 1889.2 for anatomy). Mice were stereotaxically implanted with a lightweight metal head holder under anesthesia. Before recordings, mice were gradually habituated to head restraint over several days of training following standard procedures (Crochet, 2012). On the day of recording, all whiskers except C2 were trimmed under anesthesia, and the C2 barrel column was functionally located using intrinsic signal optical imaging.

Electrophysiology

A small craniotomy (~0.5 mm) was drilled above the center of the C2 barrel column to give access for whole-cell recordings, local field potential recordings, and to allow local drug injection. For the blockade of cholinergic receptors in S1, 100 nl of atropine (2 mM) and mecamylamine (2 mM) (or each drug individually in Figure S1) were injected at subpial depths of 250, 500, and 850 μm (or 400 and 800 μm for Figure S1). Thalamic inactivation was carried out by injecting 100 nl of muscimol (1 mM) at subpial depths of 3,100 and 3,500 μm at 1.9 mm posterior and 1.5 mm lateral to Bregma. Injection of Evans Blue confirmed correct targeting of injections to the somatosensory thalamus. Whole-cell pipettes (5–8 MΩ) were filled with internal solution containing (in mM): 135 potassium gluconate, 4 KCl, 10 HEPES, 10 sodium phosphocreatine, 4 MgATP, and 0.3 Na_3GTP (adjusted to pH 7.3 with KOH). Whole-cell recordings were made with a Multiclamp 700A amplifier (Axon Instruments). Whole-cell recordings were digitized at 20 kHz by an ITC-18 analog-to-digital converter (Instrutech Corporation) under the control of IgorPro (Wavemetrics). The membrane potential (V_m) was not corrected for liquid junction potentials. All whole-cell recordings were obtained at a subpial depth ranging from 150 to 400 μm, therefore lying within L2/3. For LFP recordings a glass micropipette filled with Ringer's solution (resistance of 5–8 MΩ) was inserted into the brain to a depth of 250–350 μm. LFPs were recorded using a Multiclamp 700A amplifier and digitized at 20 kHz using an ITC-18 analog-to-digital converter under the control of IgorPro. LFP signals were band pass filtered (0.05–100 Hz).

Quantification of Whisker Movement

We filmed the C2 whisker using a high-speed (200 fps) camera in sweeps of 20–90 s duration. The mouse was illuminated from below with infrared light (850 nm). Behavioral images were synchronized to the electrophysiological recording through TTL pulses. Custom written routines running within IgorPro were used to automatically determine the whisker angle offline.

GCaMP6s Imaging of Cholinergic Axons

ChAT-Cre mice (B6.129S6-Chat$^{tm1(cre)Lowl}$/J mice, Jax 006410) were injected with a mixture of AAV1.Syn.Flex.GCaMP6s.WPRE.SV40 (Chen et al., 2013) and AAV2/9.CAG.Flex.tdTomato.WPRE.bGH (viruses made by Penn Vector Core) in the basal forebrain. In some animals only the GCaMP6s virus was injected. After 3–5 weeks of viral expression, mice were anesthetized with isoflurane and an acute imaging window (2–3 mm in diameter) was constructed, stabilized with 1.5% agarose gel and sealed with a round coverslip (4 mm). Animals were given 1–1.5 hr to recover from anesthesia in their home cage before the recording session.

Two-photon calcium imaging in layer 1 was performed essentially as previously described (Gentet et al., 2012), using a modified Sutter MOM microscope controlled by Helioscan software (Langer et al., 2013) with a MaiTai HP (Spectraphysics) femtosecond laser. Sweeps of 40 s were acquired at frame rates ranging from 8 to 20 Hz. The calcium signals were synchronized with a high-speed whisker tracking system. Acquisitions with major movement artifacts were rejected. Small motion artifacts in the xy plane were corrected by image registration using TurboReg (Thévenaz et al., 1998).

For each acquisition, regions of interest (ROIs) were drawn manually around visible horizontal axons and raw fluorescence extracted. Relative fluorescence

was calculated as $\Delta F/F_0 = (F(t) - F_0) / F_0$, where F(t) is the raw fluorescence for a given ROI in frame t and F_0 is the baseline fluorescence taken as the temporal average of the lowest quartile of the distribution of F(t).

Optogenetics

For optogenetic experiments, we used ChAT-Cre mice expressing ChR2 in a Cre-dependent manner (ChAT-Cre × LSL-ChR2) that were obtained by crossing B6.129S6-Chat$^{tm1(cre)Lowl}$/J mice (Jax 006410) with B6;129S-Gt(ROSA)26Sor$^{tm32(CAG-COP4*H134R/EYFP)Hze}$/J (Ai32, Jax 012569) (Madisen et al., 2012). Optogenetic stimulation of basal forebrain cholinergic neurons was achieved with a 300 μm optic fiber (NA 0.37, Thorlabs) coupled to a blue laser (473 nm, GMP) that provided a total light power of 6–11 mW at the output of the fiber. Light stimuli consisted of 5 s trains of 40 ms light pulses at 12 Hz. To obtain a strong cholinergic drive to S1, we targeted a region of dense S1-projecting cholinergic neurons defined by retrograde CTB labeling (0.7 mm posterior to Bregma, Figure 2A). The optic fiber was slowly lowered with a lateral angle of 10° from the vertical to avoid the lateral ventricle down to a subpial depth of 3.6 mm. The optic fiber was coupled to an 80 μm tungsten filament and at the end of recording an electrolytic lesion was made (200 μA, 8 s) to check for the correct location of the optic fiber.

Anatomy

For retrograde labeling of the cholinergic neurons projecting to the barrel cortex, we injected cholera toxin subunit B conjugated to Alexa 488 (CTB) (75 nl of 0.5% CTB at 250 and 850 μm below the pia) into the C2 barrel column of 4 ChAT-Cre mice expressing tdTomato in a Cre-dependent manner (ChAT-Cre × LSL-TdTomato) that were obtained by crossing B6.129S6-Chat$^{tm1(cre)Lowl}$/J mice with B6.Cg-Gt(ROSA)26Sor$^{tm9(CAG-tdTomato)Hze}$/J (Madisen et al., 2010). After 6–7 days, the mice were transcardially perfused with 4% paraformaldehyde (PFA). Thin (40 μm) brain sections were imaged using a confocal microscope. Alexa-488-positive cells colocalizing with tdTomato were identified, and their positions were noted in the context of a standard mouse brain atlas (Paxinos and Franklin, 2001).

To visualize the cholinergic fibers projecting to the barrel cortex, the basal forebrain of two ChAT-Cre mice were injected with 50 nl of AAV2/9.CAG.Flex.tdTomato.WPRE.bGH (Penn Vector Core). After >3 weeks for expression, the mice were transcardially perfused with 4% PFA before cutting 120-μm-thick sections for imaging.

Data Analysis and Statistics

Data were analyzed using IgorPro (Wavemetrics). Based on the whisker behavior, recording segments were classified as quiet waking (no whisker movement) or active whisking (continuous rhythmic whisker movements without object contacts). Two- or three-second time windows were used to compute mean, variance, and frequency spectra. The effect of optogenetic stimulation was measured between 1 and 4 s after the onset of the 5 s blue light pulse train, and only trials with no whisker movements were selected. The spectral analysis was carried out using a fast Fourier transform (FFT) procedure in IgorPro. The FFT magnitude was computed after subtraction of the mean, and it was normalized by the number of samples (n/2). For V_m data, the FFT was computed after removing APs with a median filter. All data are presented as mean ± SEM. Nonparametric statistical tests were used to evaluate statistical significance (Wilcoxon rank test or Wilcoxon signed rank test).

SUPPLEMENTAL INFORMATION

Supplemental Information includes three figures and can be found with this article online at http://dx.doi.org/10.1016/j.celrep.2014.11.005.

AUTHOR CONTRIBUTIONS

E.E., S.C., and C.C.H.P. designed the project. E.E. carried out and analyzed all whole-cell recordings, optogenetics, and anatomy. Y.K. and E.E. carried out and analyzed two-photon imaging experiments. S.C. and E.E. carried out and analyzed local field potential recordings. S.C. and C.C.H.P. wrote the manuscript, with comments from E.E. and Y.K.

ACKNOWLEDGMENTS

We thank the EPFL Faculty of Life Science Workshop for help with instrumentation and the Bioimaging and Optics Platform for help with microscopy. We thank Laura Fernandez, Damien Lapray, and Nadia Urbain for helpful discussions. This work was funded by grants from the Swiss National Science Foundation and the European Research Council.

Received: September 16, 2014
Revised: October 24, 2014
Accepted: November 4, 2014
Published: December 4, 2014

REFERENCES

Bakin, J.S., and Weinberger, N.M. (1996). Induction of a physiological memory in the cerebral cortex by stimulation of the nucleus basalis. Proc. Natl. Acad. Sci. USA *93*, 11219–11224.

Bennett, C., Arroyo, S., and Hestrin, S. (2013). Subthreshold mechanisms underlying state-dependent modulation of visual responses. Neuron *80*, 350–357.

Berger, H. (1929). Electroencephalogram in humans. Arch. Psychiatr. Nervenkr. *87*, 527–570.

Buzsáki, G., and Draguhn, A. (2004). Neuronal oscillations in cortical networks. Science *304*, 1926–1929.

Buzsáki, G., Bickford, R.G., Ponomareff, G., Thal, L.J., Mandel, R., and Gage, F.H. (1988). Nucleus basalis and thalamic control of neocortical activity in the freely moving rat. J. Neurosci. *8*, 4007–4026.

Chen, T.W., Wardill, T.J., Sun, Y., Pulver, S.R., Renninger, S.L., Baohan, A., Schreiter, E.R., Kerr, R.A., Orger, M.B., Jayaraman, V., et al. (2013). Ultrasensitive fluorescent proteins for imaging neuronal activity. Nature *499*, 295–300.

Chubykin, A.A., Roach, E.B., Bear, M.F., and Shuler, M.G.H. (2013). A cholinergic mechanism for reward timing within primary visual cortex. Neuron *77*, 723–735.

Crochet, S. (2012). Intracellular whole-cell patch-clamp recordings of cortical neurons in awake head-restrained mice. In Neural Network Analysis, *Volume 67*, T. Fellin and M. Halassa, eds. (New York: Humana Press), pp. 219–235.

Crochet, S., and Petersen, C.C.H. (2006). Correlating whisker behavior with membrane potential in barrel cortex of awake mice. Nat. Neurosci. *9*, 608–610.

Eggermann, E., and Feldmeyer, D. (2009). Cholinergic filtering in the recurrent excitatory microcircuit of cortical layer 4. Proc. Natl. Acad. Sci. USA *106*, 11753–11758.

Favero, M., Varghese, G., and Castro-Alamancos, M.A. (2012). The state of somatosensory cortex during neuromodulation. J. Neurophysiol. *108*, 1010–1024.

Ferezou, I., Haiss, F., Gentet, L.J., Aronoff, R., Weber, B., and Petersen, C.C.H. (2007). Spatiotemporal dynamics of cortical sensorimotor integration in behaving mice. Neuron *56*, 907–923.

Fu, Y., Tucciarone, J.M., Espinosa, J.S., Sheng, N., Darcy, D.P., Nicoll, R.A., Huang, Z.J., and Stryker, M.P. (2014). A cortical circuit for gain control by behavioral state. Cell *156*, 1139–1152.

Gentet, L.J., Avermann, M., Matyas, F., Staiger, J.F., and Petersen, C.C.H. (2010). Membrane potential dynamics of GABAergic neurons in the barrel cortex of behaving mice. Neuron *65*, 422–435.

Gentet, L.J., Kremer, Y., Taniguchi, H., Huang, Z.J., Staiger, J.F., and Petersen, C.C.H. (2012). Unique functional properties of somatostatin-expressing GABAergic neurons in mouse barrel cortex. Nat. Neurosci. *15*, 607–612.

Gil, Z., Connors, B.W., and Amitai, Y. (1997). Differential regulation of neocortical synapses by neuromodulators and activity. Neuron *19*, 679–686.

Gulledge, A.T., and Stuart, G.J. (2005). Cholinergic inhibition of neocortical pyramidal neurons. J. Neurosci. *25*, 10308–10320.

Gulledge, A.T., Park, S.B., Kawaguchi, Y., and Stuart, G.J. (2007). Heterogeneity of phasic cholinergic signaling in neocortical neurons. J. Neurophysiol. *97*, 2215–2229.

Harris, K.D., and Thiele, A. (2011). Cortical state and attention. Nat. Rev. Neurosci. *12*, 509–523.

Herrero, J.L., Roberts, M.J., Delicato, L.S., Gieselmann, M.A., Dayan, P., and Thiele, A. (2008). Acetylcholine contributes through muscarinic receptors to attentional modulation in V1. Nature *454*, 1110–1114.

Jones, B.E. (2005). From waking to sleeping: neuronal and chemical substrates. Trends Pharmacol. Sci. *26*, 578–586.

Kalmbach, A., and Waters, J. (2014). Modulation of high- and low-frequency components of the cortical local field potential via nicotinic and muscarinic acetylcholine receptors in anesthetized mice. J. Neurophysiol. *111*, 258–272.

Kilgard, M.P., and Merzenich, M.M. (1998). Cortical map reorganization enabled by nucleus basalis activity. Science *279*, 1714–1718.

Kruglikov, I., and Rudy, B. (2008). Perisomatic GABA release and thalamocortical integration onto neocortical excitatory cells are regulated by neuromodulators. Neuron *58*, 911–924.

Langer, D., van 't Hoff, M., Keller, A.J., Nagaraja, C., Pfäffli, O.A., Göldi, M., Kasper, H., and Helmchen, F. (2013). HelioScan: a software framework for controlling in vivo microscopy setups with high hardware flexibility, functional diversity and extendibility. J. Neurosci. Methods *215*, 38–52.

Lee, S.H., and Dan, Y. (2012). Neuromodulation of brain states. Neuron *76*, 209–222.

Lee, M.G., Hassani, O.K., Alonso, A., and Jones, B.E. (2005). Cholinergic basal forebrain neurons burst with theta during waking and paradoxical sleep. J. Neurosci. *25*, 4365–4369.

Lee, S., Kruglikov, I., Huang, Z.J., Fishell, G., and Rudy, B. (2013). A disinhibitory circuit mediates motor integration in the somatosensory cortex. Nat. Neurosci. *16*, 1662–1670.

Madisen, L., Zwingman, T.A., Sunkin, S.M., Oh, S.W., Zariwala, H.A., Gu, H., Ng, L.L., Palmiter, R.D., Hawrylycz, M.J., Jones, A.R., et al. (2010). A robust and high-throughput Cre reporting and characterization system for the whole mouse brain. Nat. Neurosci. *13*, 133–140.

Madisen, L., Mao, T., Koch, H., Zhuo, J.M., Berenyi, A., Fujisawa, S., Hsu, Y.W., Garcia, A.J., 3rd, Gu, X., Zanella, S., et al. (2012). A toolbox of Cre-dependent optogenetic transgenic mice for light-induced activation and silencing. Nat. Neurosci. *15*, 793–802.

Matyas, F., Sreenivasan, V., Marbach, F., Wacongne, C., Barsy, B., Mateo, C., Aronoff, R., and Petersen, C.C.H. (2010). Motor control by sensory cortex. Science *330*, 1240–1243.

McCormick, D.A., and Prince, D.A. (1986). Mechanisms of action of acetylcholine in the guinea-pig cerebral cortex in vitro. J. Physiol. *375*, 169–194.

Metherate, R., Cox, C.L., and Ashe, J.H. (1992). Cellular bases of neocortical activation: modulation of neural oscillations by the nucleus basalis and endogenous acetylcholine. J. Neurosci. *12*, 4701–4711.

O'Connor, D.H., Peron, S.P., Huber, D., and Svoboda, K. (2010). Neural activity in barrel cortex underlying vibrissa-based object localization in mice. Neuron *67*, 1048–1061.

Parikh, V., Kozak, R., Martinez, V., and Sarter, M. (2007). Prefrontal acetylcholine release controls cue detection on multiple timescales. Neuron *56*, 141–154.

Paxinos, G., and Franklin, K.B.J. (2001). The Mouse Brain in Stereotaxic Coordinates (San Diego: Academic Press).

Petreanu, L., Gutnisky, D.A., Huber, D., Xu, N.L., O'Connor, D.H., Tian, L., Looger, L., and Svoboda, K. (2012). Activity in motor-sensory projections reveals distributed coding in somatosensation. Nature *489*, 299–303.

Pfeffer, C.K., Xue, M., He, M., Huang, Z.J., and Scanziani, M. (2013). Inhibition of inhibition in visual cortex: the logic of connections between molecularly distinct interneurons. Nat. Neurosci. *16*, 1068–1076.

Pinto, L., Goard, M.J., Estandian, D., Xu, M., Kwan, A.C., Lee, S.H., Harrison, T.C., Feng, G., and Dan, Y. (2013). Fast modulation of visual perception by basal forebrain cholinergic neurons. Nat. Neurosci. *16*, 1857–1863.

Polack, P.O., Friedman, J., and Golshani, P. (2013). Cellular mechanisms of brain state-dependent gain modulation in visual cortex. Nat. Neurosci. *16*, 1331–1339.

Poulet, J.F.A., and Petersen, C.C.H. (2008). Internal brain state regulates membrane potential synchrony in barrel cortex of behaving mice. Nature *454*, 881–885.

Poulet, J.F.A., Fernandez, L.M., Crochet, S., and Petersen, C.C.H. (2012). Thalamic control of cortical states. Nat. Neurosci. *15*, 370–372.

Sachidhanandam, S., Sreenivasan, V., Kyriakatos, A., Kremer, Y., and Petersen, C.C.H. (2013). Membrane potential correlates of sensory perception in mouse barrel cortex. Nat. Neurosci. *16*, 1671–1677.

Sarter, M., Parikh, V., and Howe, W.M. (2009). Phasic acetylcholine release and the volume transmission hypothesis: time to move on. Nat. Rev. Neurosci. *10*, 383–390.

Schneider, D.M., Nelson, A., and Mooney, R. (2014). A synaptic and circuit basis for corollary discharge in the auditory cortex. Nature *513*, 189–194.

Thévenaz, P., Ruttimann, U.E., and Unser, M. (1998). A pyramid approach to subpixel registration based on intensity. IEEE Trans. Image Process. *7*, 27–41.

Wester, J.C., and Contreras, D. (2013). Differential modulation of spontaneous and evoked thalamocortical network activity by acetylcholine level in vitro. J. Neurosci. *33*, 17951–17966.

Zagha, E., Casale, A.E., Sachdev, R.N., McGinley, M.J., and McCormick, D.A. (2013). Motor cortex feedback influences sensory processing by modulating network state. Neuron *79*, 567–578.

Zhou, M., Liang, F., Xiong, X.R., Li, L., Li, H., Xiao, Z., Tao, H.W., and Zhang, L.I. (2014). Scaling down of balanced excitation and inhibition by active behavioral states in auditory cortex. Nat. Neurosci. *17*, 841–850.